

OPTIMAL CONTROL OF THE PENICILLIN G FED-BATCH FERMENTATION: AN ANALYSIS OF THE MODEL OF HEIJNEN *ET AL.*

JAN F. VAN IMPE

ESAT — Department of Electrical Engineering, and Laboratory for Industrial Microbiology and Biochemistry, Katholieke Universiteit Leuven, Kardinaal Mercierlaan 94, B-3001 Leuven, Belgium

BART M. NICOLAÏ

Department of Agricultural Engineering, Katholieke Universiteit Leuven, Leuven, Belgium

PETER A. VANROLLEGHEM

Department of Agricultural Engineering, Universiteit Gent, Gent, Belgium

JAN A. SPRIET

Department of Agricultural Engineering, Katholieke Universiteit Leuven, Leuven, Belgium

AND

BART DE MOOR AND JOOS VANDEWALLE

ESAT — Department of Electrical Engineering, Katholieke Universiteit Leuven, Leuven, Belgium

SUMMARY

This paper presents the application of optimal control theory in determining the optimal feed rate profile for the penicillin G fed-batch fermentation, using a mathematical model based on balancing methods. Since this model does not fulfil all requisites for standard optimal control, we propose a sequence of new models — that converges to the original one in a smooth way — to which the standard techniques are applicable. The unusual optimization of some initial conditions is included. We then state the conjecture that allows us to obtain the optimal control for the original model. The enormous gains in production and the vanishing of the characteristic biphasic behaviour through feed rate profile optimization raise some questions concerning the validity of this model. In this way this optimal control study can prove to be very useful for model discrimination purposes. Furthermore, mathematical and microbial insights lead to the construction of a suboptimal heuristic strategy — which we show to be a limiting case of the optimal scheme — that can serve as a basis for the development of robust, model-independent, optimal adaptive control schemes.

KEY WORDS Optimal control Non-linear systems Fed-batch fermentation processes
Biotechnological modelling

1. INTRODUCTION

The design of high-performance model-based control algorithms for biotechnological processes is hampered by two major problems which call for adequate engineering solutions. First, the process kinetics are most often poorly understood non-linear functions, while the

corresponding parameters are in general time-varying. Secondly, up till now there is a lack of reliable sensors suited to real-time monitoring of process variables which are needed in advanced control algorithms. Therefore the earliest attempts at control of a biotechnological process used no model at all. Successful state trajectories from previous runs which had been stored in the process computer were tracked using open-loop control. Many industrial fermentations are still operated using this method.

During the last two decades, two trends for the design of monitoring and control algorithms for fermentation processes have emerged.¹ In a *first* approach the difficulties in obtaining an accurate mathematical process model are ignored. In numerous papers classical methods (e.g. Kalman filtering, optimal control theory, etc.) are applied under the assumption that the model is perfectly known. Owing to this oversimplification, it is very unlikely that a real-life implementation of such controllers — very often this implementation is already hampered by e.g. monitoring problems — would result in the predicted simulation results. In a *second* approach the aim is to design specific monitoring and control algorithms without the need for a complete knowledge of the process model, using concepts from e.g. adaptive control and non-linear linearizing control. A comprehensive treatment of these ideas can be found in Reference 2 and the references cited therein.

We have shown how to combine the best of both trends into one unifying methodology for optimization of biotechnological processes: *optimal adaptive control*.^{3,4} This is motivated as follows. Model-based *optimal control* studies provide a theoretical realizable optimum. However, the real-life implementation will fail in the first place owing to modelling uncertainties. On the other hand, model-independent *adaptive controllers* can be designed, but there is *a priori* no guarantee for at least suboptimality of the results obtained. The gap between the two approaches is bridged in two steps. First, heuristic control strategies are developed with nearly optimal performance under all conditions. These suboptimal controllers are based on biochemical knowledge concerning the process and on a careful mathematical analysis of the optimal control solution. In a second step, implementation of these profiles in an adaptive model-independent way combines excellent robustness properties with nearly optimal performance.

As an example, we consider in this paper the development of a heuristic substrate feed rate controller for the penicillin G fed-batch fermentation process, based on mathematical and microbial insights. There are at least two unstructured models available in the literature that allow for the optimization of the final penicillin amount with respect to the glucose feeding rate: the model of Heijnen *et al.*⁵ and the model of Bajpai and Reuß.⁶ The latter has been analysed in References 4 and 7. The analysis in this paper is based on the unstructured mathematical model proposed by Heijnen *et al.*⁵ For the second step of the above approach, i.e. the adaptive implementation, we refer to References 3 and 4.

Nowadays penicillin G is an almost common antibiotic; nevertheless the fermentation technology and the mathematical description of the production process are still subjects of interest. The optimization of product formation during fed-batch fermentation as a part of total process control has gained renewed attention.⁸

The category of secondary metabolites includes a large number of extremely valuable compounds whose mass production has revolutionized public health in modern society. In this paper the example of penicillin G fed-batch fermentation is only used as a vehicle for presenting the basic ideas, methodology and results obtained. This fermentation process can be considered representative for the whole class of processes with secondary metabolites.⁴

The paper is organized as follows. Section 2 presents the original model of Heijnen *et al.* and the modifications to make it suitable for standard optimal control, together with the

statement of the complete optimization problem. We also formulate the basic conjecture of this paper. In Section 3 we develop for the first time the optimal feed rate profile maximizing the final amount of product, in verifying the statement by Heijnen *et al.* that *the glucose feed scheme is of crucial importance in obtaining high penicillin yields*. Section 4 presents a physical interpretation of singular control, based on a mathematical analysis of the optimal control solution. In Section 5 we derive a suboptimal strategy based on mathematical and microbial knowledge, that is found to be a useful alternative for the optimal open-loop feed rate profile. It opens perspectives for more reliable, adaptive, model-independent control schemes. Some conclusions are formulated in Section 6.

Apart from the derivation of optimal control profiles for this model — which are important on their own — we believe that the most important contributions of this paper are the following. The realizable gain due to feed profile optimization is in the region of several hundred per cent. Furthermore, the model is very sensitive towards different feeding policies. These results, together with the fact that the commonly observed biphasic behaviour of the penicillin fed-batch fermentation has disappeared after optimization, raise some questions concerning the validity of this model. In this way this optimal control study can prove to be very useful for model discrimination purposes: *optimization for model discrimination*. For more details see Reference 4. Secondly, the heuristic controllers introduced in Section 5 have an excellent performance in all cases. Moreover, since the control objective (namely to keep the specific growth rate constant during the production phase) is obtained independently of the exact analytical expressions for the specific rates, these controllers can serve indeed as a basis for the development of model-independent control algorithms. This is elaborated in detail in References 3 and 4: *optimal adaptive control*.

2. THE MODEL OF HEIJNEN *ET AL.*

2.1. The original model equations

Heijnen *et al.*⁵ used the following steps in the construction of a simple unstructured model for the penicillin G fed-batch fermentation process: (i) definition of relevant compounds in the penicillin fermentation, (ii) specification of chemical composition and specific enthalpies, (iii) formulation of elemental balances and the enthalpy balance (one of the most interesting features of this approach), (iv) formulation of mass balances for individual compounds, (v) formulation of the weight balance and (vi) selection of the kinetic equations (in this case based on a literature survey). Their research resulted in the following continuous-time model which they believe to be of great possible help in the optimization of the process:

$$\begin{aligned} \frac{dS}{dt} &= -\sigma X + u, & \frac{dX}{dt} &= \mu X, & \frac{dP}{dt} &= \pi X - k_n P \\ \frac{dG}{dt} &= \frac{1}{C_{s,in}} u - 0.0008G - 0.044r_c + 0.068r_n + 0.392r_{su} + 0.032r_o + 0.68\pi X \end{aligned} \quad (1)$$

with

S	amount of substrate (glucose) in broth (mol)
X	amount of cell mass in broth (mol dry weight)
P	amount of product (penicillin) in broth (mol)
G	total broth weight (kg)

u	substrate feed rate (mol h ⁻¹)
$C_{s,in}$	glucose concentration in feed stream (mol kg ⁻¹)
σ	specific substrate consumption rate (mol (mol dry weight) ⁻¹ h ⁻¹)
μ	specific growth rate (h ⁻¹)
π	specific production rate (mol (mol dry weight) ⁻¹ h ⁻¹)
k_h	penicillin hydrolysis constant (h ⁻¹)
r_c	net rate of CO ₂ conversion (mol h ⁻¹)
r_n	net rate of nitrogen source conversion (mol h ⁻¹)
r_o	net rate of oxygen conversion (mol h ⁻¹)
r_{su}	net rate of sulphate source conversion (mol h ⁻¹).

Observe that this model is written in a (mol, kg) unit system: concentrations of substrate, biomass and product (denoted C_s , C_x and C_p respectively) are expressed with respect to total broth weight G . In the last equation, terms with a positive sign are due to the input of glucose, nitrogen source, sulphate source, oxygen and precursor respectively. Terms with a negative sign represent evaporation and carbon dioxide production respectively. For more details see Reference 5. The specific rates σ , μ and π are modelled as follows.

1. The specific substrate consumption rate σ is modelled using a Monod-type relationship⁹

$$\sigma = Q_{s,max} \frac{C_s}{K_s + C_s} \quad (2)$$

with

$Q_{s,max}$ maximum specific sugar uptake rate (mol (mol dry weight)⁻¹ h⁻¹)
 K_s Monod constant for sugar uptake (mol kg⁻¹).

2. The specific production rate π is assumed to be directly coupled with the specific growth rate μ , following a Blackman-type relation⁹

$$\pi(\mu) = Q_{p,max} \begin{cases} \mu/\mu_{crit} & \text{for } \mu \leq \mu_{crit} \\ 1 & \text{for } \mu \geq \mu_{crit} \end{cases} \quad (3)$$

with

$Q_{p,max}$ maximum specific production rate (mol (mol dry weight)⁻¹ h⁻¹)
 μ_{crit} critical specific growth rate (h⁻¹).

3. The (overall) specific growth rate μ is given by

$$\mu = Y_{x/s}(\sigma - m - \pi/Y_{p/s}) \quad (4)$$

with

m overall specific maintenance demand (mol (mol dry weight)⁻¹ h⁻¹)
 $Y_{x/s}$ biomass-on-substrate yield coefficient (mol dry weight mol⁻¹)
 $Y_{p/s}$ product-on-substrate yield coefficient (mol mol⁻¹)

which represents an *endogenous* metabolism viewpoint. This means that the energy supply for maintenance of living biomass and for product synthesis is assumed to be due to combustion of part of the biomass.

Table I shows the parameters and initial conditions used in all simulations; α is the total amount of substrate available for fermentation. The expressions for the rates r_c , r_n , r_o and r_{su} can be found in Reference 5.

Table I. Parameters and initial conditions used in simulations

Parameters				Initial conditions			
$Q_{s,max}$	0.0245	$Q_{p,max}$	$3.3 \cdot 10^{-4}$	X_0	4000	S_0	To be specified
K_s	0.0056	μ_{crit}	0.01	P_0	0	G_0	$98020 + S_0/C_{s,in}$
$Y_{x/s}$	3.67	k_h	0.002	t_0	0	α	205500
$Y_{p/s}$	0.46	$C_{s,in}$	1/0.36				
m	0.0034						

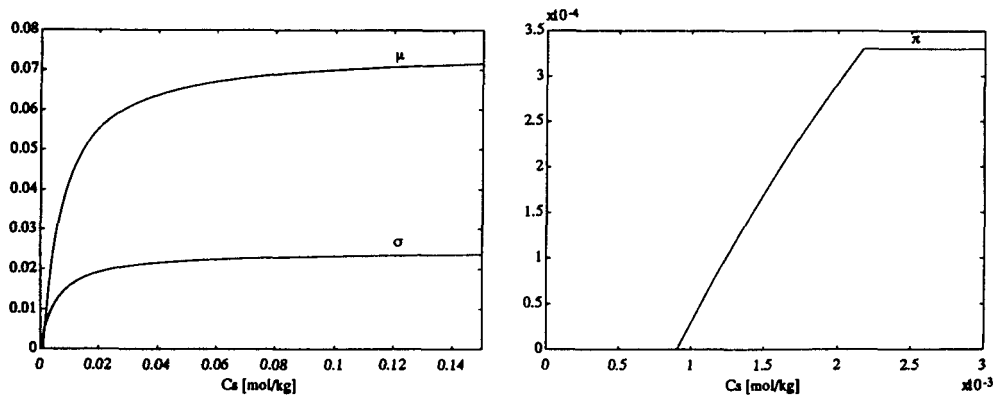
The specific substrate consumption rate σ in (2) is a function of C_s only. Substitution of model equations (2) and (3) in model equation (4) delivers an implicit relationship between μ and C_s , the solution for μ of which can be used in equation (3). We conclude that the three *specific rates* σ , μ and π are functions of C_s only. Figure 1 shows the results of these manipulations. Since π has a discontinuity in the derivative with respect to μ at $\mu = \mu_{crit}$, it is quite clear that π as a function of C_s exhibits a corner at the corresponding value of C_s , say $C_{s,crit}$. Notice that both the (overall) specific growth rate μ and the specific production rate π become zero at a positive value of substrate concentration C_s . Obviously, this is due to the endogenous metabolism assumption. As a result, these kinetics represent a degenerate version of a fermentation process characterized by a *monotonic specific growth rate* μ and a *non-monotonic specific production rate* π .^{4,10} They can also be interpreted as a degenerate case of a *fermentation process with growth-associated product formation*.

2.2. A simplified weight balance

We now show that on the right-hand side of differential equation (1) for total broth weight G all terms except the first one (which represents the input of glucose) have negligible influence on the dynamics and final value of the product P . This can be seen as follows. Since all specific rates are functions of C_s only, it is useful to derive the differential equation for C_s :

$$\frac{dC_s}{dt} = \frac{1}{G} \frac{dS}{dt} - \frac{C_s}{G} \frac{dG}{dt}$$

For π out of saturation, typical orders of magnitude are $C_s = O(10^{-3})$, $\mu = O(10^{-3})$ and

Figure 1. Specific rates σ , μ and π as functions of C_s

$\pi = O(10^{-4})$. Using the exact expressions for the specific rates r_c , r_n , r_o and r_{su} (see Reference 5) on the right-hand side of equation (1), it can be verified that under these conditions the second most important contribution comes from the term representing evaporation. Thus the above dynamic equation for C_s can be written as

$$\frac{dC_s}{dt} = -\sigma C_x + \left(1 - \frac{C_s}{C_{s,in}}\right) \frac{u}{G} + 0.0008C_s + \text{lower-order terms}$$

With u of the order of magnitude of 1000 mol h^{-1} , the term $0.0008C_s$ has negligible influence on the dynamics of C_s and thus on the dynamics of all specific rates.

Thus, in optimizing the final product amount $P(t_f)$ with respect to the glucose feeding policy, we will omit all these terms to simplify the analytical developments. The original model then reduces to

$$\frac{dS}{dt} = -\sigma X + u, \quad \frac{dX}{dt} = \mu X, \quad \frac{dP}{dt} = \pi X - k_h P, \quad \frac{dG}{dt} = \frac{1}{C_{s,in}} u \quad (5)$$

Another advantage of this model structure is that we can take care of an isoperimetric constraint on the input *without* introducing an additional state equation.

As an example, using $S_0 = 5500 \text{ mol}$ and a constant input $u = 1000 \text{ mol h}^{-1}$ for 200 h, we obtain $P(t_f) = 3001.12 \text{ mol}$ on using the complete equation for G in (1), but a value which is only 0.03% smaller on using only the first term as in (5). The simulation results using the simplified model are shown in Figure 2. Some comments are in order here.

1. Up to now the penicillin fermentation — when operated in fed-batch mode — is most often classified in the group of product formation processes of the non-growth-associated type. In agreement with the experimentally observed behaviour, the process is assumed to consist of two phases: a phase of rapid growth with almost no product formation (*trophophase*) and a phase with limited growth in which the product is formed (*idiophase*). The simulation results for $C_s(t)$, $C_x(t)$ and $P(t)$ are obviously in agreement with this biphasic description. However, Heijnen *et al.* obtained these results on the assumption of a direct coupling between specific growth rate and specific rate of product formation (see equation (3)). The μ - and π -profiles in Figure 2 illustrate some of these ideas. Heijnen *et al.* therefore concluded that *the apparent separation between*

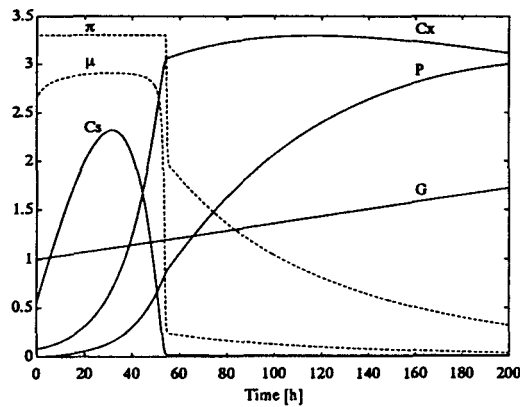


Figure 2. Constant glucose feed rate and corresponding cell, glucose, product, μ - and π -profiles. Scaling: $C_s \times 10$, $C_x \times 2$, $P/10^3$, $G/10^5$, $\mu \times 40$, $\pi \times 10^4$

production and growth phases does not necessarily mean that penicillin production is of the non-growth-associated type.

2. Another feature of the simulation results is an apparent *lag phase* in the penicillin production curve of about 20 h. Observe that this was not introduced *a priori* in the model. Heijnen *et al.* concluded that it remains possible that there is in reality no real lag in the beginning of penicillin production.
3. Another modelling approach that has been followed is the assumption of a *relationship between mycelial age and its productivity*. Most often the product activity is assumed to decrease at high mycelial age.¹¹ In this way the decreasing π -curve (Figure 2) during the production phase can be modelled. However, Heijnen *et al.* did not model such an age dependence. In their viewpoint the decreasing π -profile may very well be explained either by dilution due to increasing broth weight or by hydrolysis of penicillin to penicilloic acid.

Heijnen *et al.* concluded that with their growth-coupled penicillin production most of the phenomena observed in practice — which have often led to the assumption of non-growth-associated or age-dependent penicillin productivity — can be adequately described. We will come back to these interpretations in subsequent sections. However, from the mathematical point of view the commonly observed separation between growth and production phases is quite a useful feature in optimizing the process.

2.3. Statement of the optimization problem

Heijnen *et al.*⁵ used their model to illustrate that the *feed rate profile during fermentation is of vital importance in the realization of a high production rate throughout the duration of the fermentation*. This statement was based on the following set of controls for 200 h: (i) a constant input $u(t) = 1000 \text{ mol h}^{-1}$ (the results of which are shown in Figure 2), (ii) a linearly increasing input $u(t) = 500 + 5t \text{ mol h}^{-1}$ and (iii) a linearly decreasing input $u(t) = 1500 - 5t \text{ mol h}^{-1}$. The initial substrate amount was fixed at $S_0 = 5500 \text{ mol}$. Using the simplified model, we obtain $P(t_f) = 3001, 5883$ and 89 mol respectively. Although Heijnen *et al.* did not consider other feeding strategies in an attempt to obtain the optimal substrate feeding profile, the above results indicate that the present model allows indeed for the optimization of the final amount of product, $P(t_f)$, with respect to the glucose feed rate scheme.

We now formulate the problem of optimizing the final product amount as an optimal control problem. With the definitions (superscript T denotes the transpose of a vector)

$$\begin{aligned} \mathbf{x} &= (x_1 \ x_2 \ x_3 \ x_4)^T \triangleq (S \ X \ P \ G)^T \\ \mathbf{f} &= (f_1 \ f_2 \ f_3 \ f_4)^T \triangleq (-\sigma X \ \mu X \ \pi X - k_h P \ 0)^T \\ \mathbf{b} &= (b_1 \ b_2 \ b_3 \ b_4)^T \triangleq (1 \ 0 \ 0 \ 1/C_{s,in})^T \end{aligned}$$

we obtain the following state space model linear in the control u :

$$\frac{d\mathbf{x}}{dt} = \mathbf{f}(\mathbf{x}) + \mathbf{b}u \quad (6)$$

Numerical values for the initial conditions are given in Table I. $x_2(0)$ and $x_3(0)$ are given; the initial amount of substrate, $x_1(0)$, is *free*. $x_1(0)$ and $x_4(0)$ are related by

$$x_4(0) = G_* + x_1(0)/C_{s,in} \quad (7)$$

where G_* denotes the given initial weight *without* substrate ($G_* = 98\,020 \text{ kg}$ (Table I)).

The optimization problem is to determine for the given set of differential equations (6) the optimal initial state \mathbf{x}_0^* and the optimal feed rate profile $u^*(t)$ that minimize the performance index

$$J[u, \mathbf{x}_0] = g[\mathbf{x}(t_f)] \triangleq -x_3(t_f) \quad (8)$$

i.e. maximize the final amount of product, subject to the following constraints.

- (i) $t_0 = 0$, t_f is free.
- (ii) All variables have to be kept positive:

$$\forall t \in [0, t_f]: x_i(t) \geq 0 \quad \text{for } i = 1, \dots, 4 \quad \wedge \quad u(t) \geq 0$$

- (iii) The total amount of substrate available, α , is fixed, i.e.

$$x_1(0) + \int_{t_0}^{t_f} u(t) dt = \alpha \quad (9)$$

The last *isoperimetric* constraint on the input is equivalent to a *physical* constraint of the form (see the simplified differential equation for total broth weight G in (5))

$$x_4(t_f) \equiv G(t_f) = G_f, \quad G_f \text{ fixed} \quad (10)$$

2.4. The basic conjecture

As can be easily seen from model equation (3) and Figure 1, the specific production rate π exhibits a *corner* at $\mu = \mu_{\text{crit}}$ or equivalently at $C_s = C_{s,\text{crit}}$. As a result, some partial derivatives $\partial f_i / \partial x_j$ are not continuous. Thus we cannot apply standard optimal control theory.^{12,13} To circumvent this problem, we replace the piecewise smooth Blackman-type kinetics $\pi(\mu)$ in (3) by a family of completely smooth curves that converges as a function of one parameter to the original kinetics. This is basically inspired by the following conjecture.

Conjecture 1

Suppose we have a convergent sequence of models $\{\mathcal{M}(\mathbf{p})\}$, where \mathbf{p} is a set of parameters

$$\lim_{\mathbf{p} \rightarrow \mathbf{p}_0} \mathcal{M}(\mathbf{p}) \triangleq \mathcal{M}_0$$

Suppose that for every model $\mathcal{M}(\mathbf{p})$ with $\mathbf{p} \neq \mathbf{p}_0$ we can determine the optimal control $u(\mathbf{p}, t)$ that minimizes some cost index $J[u]$ with standard optimal control theory. Then the sequence of optimal controls $\{u(\mathbf{p}, t)\}$ is convergent:

$$\lim_{\mathbf{p} \rightarrow \mathbf{p}_0} u(\mathbf{p}, t) \triangleq u_0(t)$$

Moreover, this limit $u_0(t)$ is the optimal control for model \mathcal{M}_0 minimizing $J[u]$.

It can be easily illustrated that proving Conjecture 1 *in general* is not possible. In Reference 4 we give an outline of the proof if some *additional assumptions* are satisfied. However, it may be very difficult in practice to verify all these assumptions.

Because at this time more general results are still lacking, we can proceed as follows for a particular optimal control problem characterized by a model \mathcal{M}_0 . We *assume a priori* that Conjecture 1 holds. Then we select a model $\mathcal{M}(\mathbf{p}_n)$ *sufficiently close* to the limit model \mathcal{M}_0 , i.e. we choose n sufficiently large. If we are able to determine the optimal control solution

using model $\mathcal{M}(\mathbf{p}_n)$, then this solution will be at least an excellent approximation for the optimal control to the limit model \mathcal{M}_0 . In the following it will be illustrated that the validity of Conjecture 1 can always be verified *a posteriori*.

2.5. A modified model

Consider the following relationship between μ and π , a Dabes-type kinetics,⁹ with parameters A and B :

$$\mu = A\pi + \frac{B\pi}{Q_{p,\max} - \pi} \quad (11)$$

or, in another way,

$$A\pi^2 - (Q_{p,\max}A + B + \mu)\pi + Q_{p,\max}\mu = 0$$

Solving this quadratic equation for π and taking the root with negative sign — we want $\pi = 0$ at $\mu = 0$ as in the original kinetics (3) — leads to

$$\pi(\mu) = \frac{Q_{p,\max}A + B + \mu - \sqrt{[(Q_{p,\max}A + B + \mu)^2 - 4AQ_{p,\max}\mu]}}{2A}$$

We now eliminate one parameter, say A , by solving

$$\frac{d\pi}{d\mu} (\mu = 0) = \frac{Q_{p,\max}}{\mu_{\text{crit}}}$$

which imposes that the derivative of π at $\mu = 0$ must be equal to the value derived from equation (3). The solution is

$$A = \frac{\mu_{\text{crit}} - B}{Q_{p,\max}}$$

and thus we obtain

$$\pi(\mu) = Q_{p,\max} \frac{\mu + \mu_{\text{crit}} - \sqrt{[(\mu + \mu_{\text{crit}})^2 - 4(\mu_{\text{crit}} - B)\mu]}}{2(\mu_{\text{crit}} - B)} \quad (12)$$

which is the desired family of smooth curves, where B , which must lie in the range $0 < B < \mu_{\text{crit}}$, is the only parameter.

Let us consider now the boundaries for the parameter B . For $B \rightarrow \mu_{\text{crit}}$, A tends to zero and the above equation becomes undetermined. However, solving the original relation (11) for π with $A = 0$ delivers the Monod-type law

$$\pi(\mu) = Q_{p,\max} \frac{\mu}{\mu_{\text{crit}} + \mu} \quad (13)$$

which is of course also a completely smooth relationship. On the other hand, as $B \rightarrow 0$, equation (12) reduces to

$$\pi(\mu) = Q_{p,\max} \frac{\mu + \mu_{\text{crit}} - \sqrt{[(\mu - \mu_{\text{crit}})^2]}}{2\mu_{\text{crit}}} = \frac{Q_{p,\max}}{2\mu_{\text{crit}}} (\mu + \mu_{\text{crit}} - |\mu - \mu_{\text{crit}}|)$$

which is in fact another form of the original model (3). Thus we can refine the boundaries for B to $0 < B \leq \mu_{\text{crit}}$.

We conclude that we have constructed a one dimensional family of curves — and thus a

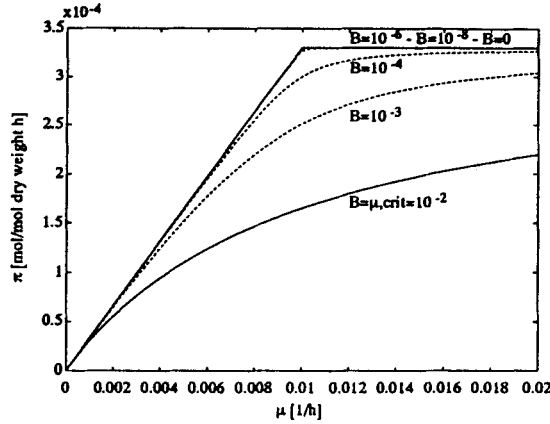


Figure 3. Dabes-type kinetics $\pi(\mu)$ for various values of parameter B

family of models — that is completely smooth within the given boundaries of the parameter B , thus assuring the continuity of $\partial f_i / \partial x_j$ for all i and j . Moreover, as $B \geq 0$, we come arbitrarily close to the original model. In Figure 3 we show some members of the family (12) for different values of B . From the numerical point of view, setting $B = 10^{-11}$ in equation (12) is a very accurate approximation in simulating the original Blackman-type kinetics (3).

Obviously, we can now determine the optimal control $u^*(B, t)$ for every B within the given boundaries $]0, \mu_{\text{crit}}]$ using standard optimal control theory. For the original model — corresponding to $B = 0$ — we will make use of Conjecture 1.

Observe that from a mathematical point of view the approximation of the piecewise smooth Blackman-type kinetics (3) can be done by any family of completely smooth curves that converges to the original kinetics. Clearly, the optimal control solution for the original kinetics is independent of this choice. However, from a biochemical point of view a sharp corner in π at $\mu = \mu_{\text{crit}}$ must be considered as a first approximation of real-life fermentation conditions. By using Dabes-type kinetics, each model of the sequence $\{\mathcal{M}_n\}$ can be assigned a meaningful interpretation.

3. OPTIMAL CONTROL USING THE MODIFIED MODEL

3.1. Solution of the two-point boundary value problem

The given optimization problem can be formulated within the frame of the minimum principle^{12,13} as a *two-point boundary value problem* (TPBVP). The Hamiltonian \mathcal{H} for this problem is

$$\begin{aligned} \mathcal{H} &= \lambda^T [\mathbf{f}(\mathbf{x}) + \mathbf{b}u] \triangleq \phi + \psi u \\ \phi &= \lambda_1 f_1 + \lambda_2 f_2 + \lambda_3 f_3, \quad \psi = \lambda_1 + \lambda_4 / C_{s,\text{in}} \end{aligned} \quad (14)$$

The adjoint vector λ satisfies the following system of differential equations:

$$\frac{d\lambda}{dt} = -\frac{\partial \mathcal{H}}{\partial \mathbf{x}} = -\frac{\partial \mathbf{f}^T}{\partial \mathbf{x}} \lambda \quad (15)$$

Note that in order to compute $\partial f_i / \partial x_1$ and $\partial f_i / \partial x_4$, $i = 2, 3$, we need $\partial \mu / \partial x_1$ and $\partial \mu / \partial x_4$. These

can be obtained by substituting equation (12) in equation (4) and calculating the *implicit* partial derivatives with respect to x_1 and x_4 respectively.

The state equations (6) together with the costate equations (15) constitute a set of 2×4 first-order differential equations. The required boundary conditions are as follows.

- (i) $x_2(0)$ and $x_3(0)$ are given.
- (ii) $x_1(0)$ and $x_4(0)$ are interrelated by equation (7).
- (iii) Since $x_1(0)$ and $x_4(0)$ are not given explicitly, it can be shown that the following condition must be satisfied:⁴

$$\lambda_1(0) + \lambda_4(0)/C_{s,in} = \psi(0) = 0$$

- (iv) $x_4(t_f)$ is given by equation (10).
- (v) $\lambda_i(t_f)$, $i = 1, \dots, 3$, are given by

$$\lambda_i(t_f) = \frac{\partial g}{\partial x_i} [\mathbf{x}(t_f)]$$

or, using (8),

$$(\lambda_1(t_f) \ \lambda_2(t_f) \ \lambda_3(t_f))^T = (0 \ 0 \ -1)^T \quad (16)$$

As stated in the minimum principle, an *extremal* control follows from the minimization of the Hamiltonian \mathcal{H} in (14) over all *admissible* control functions while satisfying the given TPBVP:

$$\min_{\text{all admissible } u} \mathcal{H}(\mathbf{x}^*, \boldsymbol{\lambda}^*, u) = \mathcal{H}(\mathbf{x}^*, \boldsymbol{\lambda}^*, u^*)$$

Note that since all conditions are *necessary* conditions, we can only obtain *extremal* solutions $(\mathbf{x}^*, \boldsymbol{\lambda}^*, u^*)$ which must be checked for optimality. Because the state equations (6) and the cost index (8) are time-invariant, the Hamiltonian \mathcal{H} remains constant along an extremal trajectory. Since the final time t_f is free, we know that $\mathcal{H} = 0$.

As already mentioned, the original kinetics (2)–(4) represent a degenerate case of a fermentation process with monotonic specific growth rate μ and non-monotonic specific production rate π — the corner point is a degenerate maximum — for which an efficient computational algorithm yielding the optimal control has been derived in Reference 4. However, the original model is only piecewise smooth, so this algorithm cannot be used directly because it requires the computation of the partial derivatives (up to second order) of the right-hand side of model equations (6) with respect to the state.

We verify now that the computational algorithm can be used for any model with a specific production rate kinetics within the family of completely smooth curves (12). The optimal solution using the original model is then obtained by considering the limit

$$\lim_{B \geq 0} u^*(B, t) \triangleq u^*(B = 0, t)$$

as stated in Conjecture 1.

Because the Hamiltonian \mathcal{H} is *linear* in the control input u , the minimum principle fails to provide the solution on any singular interval $[t_i, t_{i+1}]$ where the function ψ remains zero. It has been shown⁴ that this problem is a singular problem of order two. In that case the singular control can be calculated by solving

$$\frac{d^2\psi}{dt^2} = 0$$

for the control input u . We obtain

$$u_{\text{sing}}(t) = \frac{\lambda^T [(\partial f / \partial \mathbf{x}) \mathbf{d} - (\partial \mathbf{d} / \partial \mathbf{x}) \mathbf{f}]}{\lambda^T (\partial \mathbf{d} / \partial \mathbf{x}) \mathbf{b}} \quad (17)$$

with

$$\mathbf{d} \triangleq -\frac{\partial \mathbf{f}}{\partial \mathbf{x}} \mathbf{b}$$

It can be verified that for all kinetics (12) the denominator of the singular control $u_{\text{sing}}(t)$ is different from zero. Since both the numerator and the denominator are *linear* in the costate variables λ and there exist three linear homogeneous equations between them, we know that the optimal control along a singular arc is a *non-linear feedback law of the state variables x only*. These three equations are

$$\psi \equiv \lambda^T \mathbf{b} = 0, \quad \frac{d\psi}{dt} \equiv \lambda^T \mathbf{d} = 0, \quad \phi \equiv \lambda^T \mathbf{f} = 0$$

For this problem it can be seen that λ_4 has disappeared from $u_{\text{sing}}(t)$, since $f_4 \equiv 0$. Thus the first equation can be omitted and the last two can be solved as

$$\begin{pmatrix} f_1 & f_2 \\ \beta_1 & \beta_2 \end{pmatrix} \begin{pmatrix} \lambda_1 \\ \lambda_2 \end{pmatrix} = - \begin{pmatrix} f_3 \\ \beta_3 \end{pmatrix} \lambda_3$$

$$\beta_i \triangleq b_1 \frac{\partial f_i}{\partial x_1} + b_4 \frac{\partial f_i}{\partial x_4}, \quad i = 1, \dots, 3$$

Consider the case of an unbounded input u and an unconstrained state vector \mathbf{x} . As shown in Reference 4, the problem then reduces to the *two-dimensional optimization of the initial amount of substrate S_0 and the time instant t_2 at which the switch from batch to singular control occurs*, the optimal control sequence being *batch–singular arc–batch*. The following straightforward computational algorithm has been proposed.^{4,14}

Algorithm

Step 1. Make a guess of S_0 or, equivalently, determine the amount of substrate, α_{growth} , consumed during the growth phase.

Step 2. Make a guess of t_2 . Integrate the state equations (6) from $t = 0$ to $t = t_2$ with $u(t) = 0$. This completes the *growth* phase.

Step 3. Integrate the state equations (6) using the above-determined singular control (17) until all substrate available, α in (9), is added or, equivalently, until the bioreactor is completely filled (equation (10)) at time $t = t_3$.

Step 4. Complete the integration with $u(t) = 0$ until the stopping condition — depending on the cost index — is satisfied at time $t = t_f$. This completes the *production* phase. Store the value of the cost index $J[u, \mathbf{x}_0]$ in (8).

Step 5. Repeat Steps 2–4 considering $t_{2,\text{new}} = t_{2,\text{old}} \pm \delta t$, with δt as small as required. Save the time t_2 at which the cost index $J[u, \mathbf{x}_0]$ in (8) reaches its minimum.

Step 6. Repeat Steps 1–5 with a new guess of S_0 in order to minimize $J[u, x_0]$.

For the performance measure under consideration, equation (8), it can be easily shown (by using (14) and (16)) that the stopping condition for this case is $dP/dt(t_f) = 0$, as could be expected. In the case of a constraint on the control u and/or the state vector x , only some minor modifications are required, the algorithm itself remaining a two-dimensional search. A detailed analysis of this algorithm in comparison with the algorithm proposed by Lim *et al.*¹⁵ together with a verification of all necessary conditions for optimality can be found in Reference 4. The main difference from the algorithm of Lim *et al.* is that we do not make use of the costate variables, whatever the performance index under consideration.

3.2. Simulation results

We now present some results obtained with the above computational algorithm. We concentrate on two specific values of the parameter B : (i) $B = 10^{-11}$ as an approximation of the original Blackman-type kinetics (3) and (ii) the other extremal value $B = \mu_{crit} = 10^{-2}$, where $\pi(\mu)$ reduces to the Monod-type law (13).

3.2.1. $B = 10^{-11}$. In the left plot of Figure 4 we have visualized the actions taken by the computational algorithm for $B = 10^{-11}$. For every S_0 the optimal switch time t_2 has been calculated. As a consequence, we obtain the corresponding values for $P(t_f)$ and t_f . Clearly, the optimal couple (S_0^*, t_2^*) is the one which maximizes $P(t_f)$. Observe the quadratic behaviour of $P(t_f)$ as a function of S_0 , so that there exists a *unique optimal solution* to this problem.

Observe that there exists a lower limit S_{min} on the possible values for S_0 , corresponding to $t_2 = 0$. In that case the complete initial state x_0 is on the singular hyperplane, so singular control starts immediately. Note that $S_0 = \alpha$ corresponds to a complete *batch* fermentation: $t_f \equiv t_3 \equiv t_2$, with $u(t) = 0$ for all t . Even for values of S_0 in the neighbourhood of α , the condition $dP/dt = 0$ is never met *before* $t = t_2$. As a result, we can indeed apply the proposed computational algorithm to the whole possible range $S_0 \in [S_{min}, \alpha]$. A derived benefit is of course that *a good starting value for S_0 is not required for the algorithm to converge*. Some numerical values for the optimal control are summarized in Table II. The right plot of Figure 4

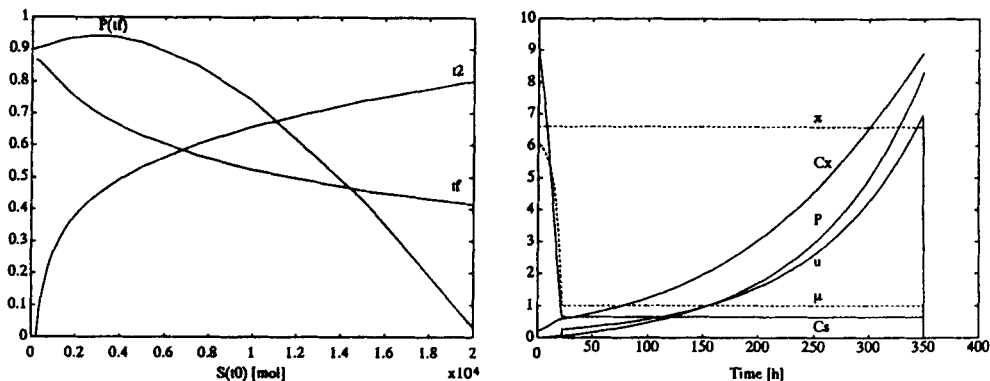


Figure 4. $B = 10^{-11}$. Left plot: extremal values for $P(t_f)$, t_2 and t_f as functions of S_0 . Scaling: $t_f/50$, $t_f/500$, $(P(t_f) - 8150)/180$. Right plot: optimal glucose feed rate and corresponding cell, glucose, product, π - and μ -profiles. Scaling: $C_s \times 300$, $C_x \times 5$, $P/10^3$, $\mu \times 100$, $\pi \times 2 \times 10^4$, $u/300$

Table II. Optimal and suboptimal control results

	$\mu(t_2)$	S_0	t_2	t_3	t_f	P_f	$P_f/P_{f,\text{optimal}}$
$B = 10^{-11}$							
Optimal control	Optimal	3000	22·321	349·987	350·101	8319·461	1·0000
Heuristic control	μ_{crit}	3000	22·337	350·037	350·151	8319·239	0·9999
$B = 10^{-2}$							
Optimal control	Optimal	326	0	277·205	277·320	4564·455	1·0000
Heuristic control	Optimal	1000	12·225	304·665	304·792	4553·437	0·9976
Heuristic control	μ_{crit}	7000	29·573	292·890	292·995	4399·589	0·9639

shows the corresponding time profiles. Let us make the following remarks.

1. From Table II we note that the optimal initial substrate amount S_0 is rather low as compared with the total amount available, $\alpha = 205\,500$ mol, resulting in a small first batch phase $[0, t_2]$ of 22·32 h. In fact, the singular interval $[t_2, t_3]$ takes most of total fermentation time t_f . The terminating batch phase $[t_3, t_f]$ is negligibly small.
2. From the profiles for $C_x(t)$ and $P(t)$ (Figure 4) we conclude that although the optimal control algorithm is based on the conjecture of a *biphasic* process, this biphasic behaviour has disappeared almost completely as compared with e.g. the results for the *constant* strategy of Figure 2. Principally this is due to the structure of the specific production rate π in (3), which represents a direct coupling between product synthesis and biomass growth.
3. On the singular arc $[t_2, t_3]$ the optimal control seems to maintain μ at the lowest possible value ($\mu \approx \mu_{\text{crit}}$) which still guarantees the maximum possible value for π . We have shown in Reference 4 that during singular control $C_s(t)$ (and thus $\mu(t)$ and $\pi(t)$) is time-varying, since $k_h \neq 0$. However, k_h is so small that the resulting variations in C_s (and thus in μ and π) are in fact negligible, so that they cannot be detected on this plot.
4. It is important to see that the optimal control keeps π on its maximum value for all $t < t_3$. This will be at the basis of *suboptimal* profiles presented in Section 5.
5. In order to evaluate the performance of the optimal control $u^*(t)$, we need some *reference*. Since we do not penalize the total fermentation time t_f in the cost index $J[u, \mathbf{x}_0]$ in (8), a good choice might be the outcome of a *constant* control with $t_f = t_f^*$, t_f^* denoting the optimal fermentation time. For convenience we take $S_{0,\text{ref}} = 0$ mol. Then we define the *gain* \mathcal{G} (%) as

$$\mathcal{G} \triangleq 100 \times \frac{J[u^*, \mathbf{x}_0^*] - J[u_{\text{ref}}, \mathbf{x}_{0,\text{ref}}](t_f = t_f^*)}{J[u_{\text{ref}}, \mathbf{x}_{0,\text{ref}}](t_f = t_f^*)} \%$$

For $B = 10^{-11}$ a constant control for 350·101 h with $S_0 = 0$ produces 1981·283 mol penicillin. Thus for the optimal control $u^*(t) \equiv u^*(B = 0, t)$ we obtain a *gain* $\mathcal{G} = 319·9\%$. Consider now a constant feed rate strategy. Optimizing the initial substrate amount S_0 and the final time t_f leads to $S_0 = 90·156$ mol, $t_f = 129·688$ h and $P_f = 3779·012$ mol. Observe that this optimal final amount is still far away from the optimal control result. From this simple parametric optimization we can conclude that *this model is very sensitive towards different feeding policies*.

Observe the enormous increase in the final product amount $P(t_f)$, which may suggest some

questions concerning the validity of the model of Heijnen *et al.*⁵ under conditions imposed by applying the optimal feed rate. Since up to now the penicillin fermentation has been recognized through all experiments as an intrinsically *biphasic* process, it seems unlikely that the obtained control put into practice would result in a quasi-*monophasic* fermentation while producing such a high gain. We conclude that the results obtained using optimal control theory suggest some possible shortcomings in this model: *optimization for model discrimination*. A deeper study of this model in comparison with the model of Bajpai and Reuß⁶ can be found in Reference 4.

3.2.2. $B = \mu_{crit} = 10^{-2}$. We now give the analogous results for the other extremal value $B = \mu_{crit} = 10^{-2}$ in order to demonstrate that the computational algorithm can be applied to *every* model with $0 < B \leq \mu_{crit}$. The left plot of Figure 5 shows the evolution of t_2 and thus $P(t_f)$ and t_f as functions of S_0 . Observe that the optimal couple (S_0^*, t_2^*) corresponds to $t_2 = 0$; in other words, the optimal initial state lies on the singular hyperplane itself. As a consequence, the separation between growth and production phases has disappeared completely. This is also illustrated by the time profiles of the right plot of Figure 5. In this case both σ and π are of Monod type: the corner point in π has disappeared completely (see Figure 3). However, the optimal solution does *not* consist of adding all substrate available at $t = 0$ followed by a batch phase as could be expected at first sight. The main reason is the following. Combining equations (2) and (4) with (13), we can verify that the resulting expression for π as a function of C_s does not satisfy an equation of the form

$$\pi(C_s) = Y_{p/x}\mu(C_s)$$

In other words, this is not a case of completely growth-associated production.

For this value of B the lower limit S_{min} is equal to the optimal value S_0^* . Note again that the condition $dP/dt = 0$ is never met *before* $t = t_2$, so we can indeed apply the proposed algorithm to the whole interval $S_0 \in [S_{min}, \alpha]$. Some numerical values for the optimal control are summarized in Table II.

Observe that on the singular arc the variations in π and μ (and thus in C_s) with respect to time are more pronounced than in the case of $B = 10^{-11}$, although k_h has not been changed. We conclude that the *model structure* itself also plays an important role in the amplitude of these variations.

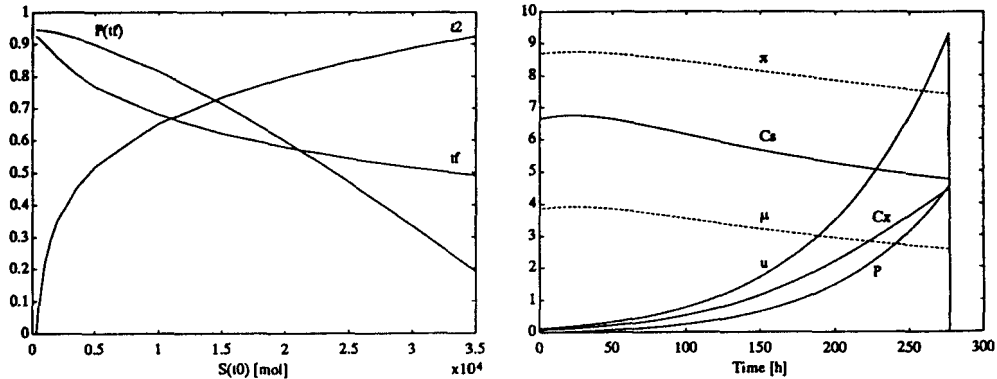


Figure 5. $B = \mu_{crit} = 10^{-2}$. Left plot: extremal values for $P(t_f)$, t_2 and t_f as functions of S_0 . Scaling: $t_2/50$, $t_f/300$, $(P(t_f) - 4300)/280$. Right plot: optimal glucose feed rate and corresponding cell, glucose, product, π - and μ -profiles. Scaling: $C_s \times 2 \times 10^3$, $C_x \times 2$, $P/10^3$, $\mu \times 200$, $\pi \times 4 \times 10^4$, $u/300$

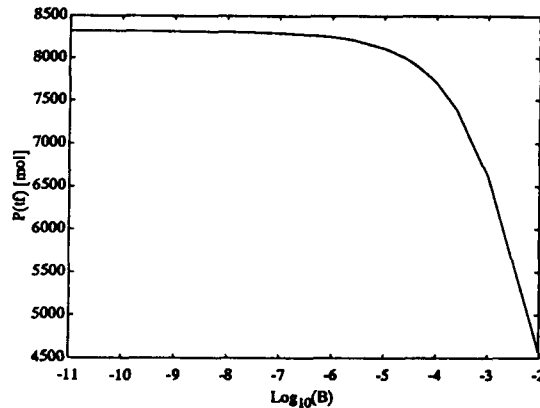


Figure 6. Optimal production $P(t_f)$ as a function of B

A constant strategy for 277–320 h with $S_0 = 0$ mol produces 1978·425 mol penicillin, so the gain using the optimal control is $\mathcal{G} = 130\cdot7\%$.

3.2.3. $0 < B \leq \mu_{crit}$. As already mentioned, we can repeat these calculations for every B within the given boundaries. The result for the optimal production $P(t_f)$ as a function of parameter B is shown in Figure 6 as an illustration of Conjecture 1. From this plot we conclude that the sequence of optimal controls $u^*(B, t)$ is indeed convergent. Note also that for $B < 10^{-9}$ the cost has almost reached its limit value.

4. PHYSICAL INTERPRETATION OF SINGULAR CONTROL

In Reference 4 the following theorem is proven for the performance index (8): *if the specific rates σ , μ , and π are functions of substrate concentration C_s only, with continuous derivatives up to second order, then during singular control the substrate concentration remains constant if and only if the product decay constant k_h equals zero. This constant value maximizes the ratio π/σ .*

We have already pointed out that the three specific rates σ in (2), π in (3) and μ in (4) are functions of substrate concentration C_s only. However, owing to the corner point in π , these kinetics are *not* continuously differentiable for every value of C_s . As a result, the above theorem cannot be used to characterize the singular control arc when using the original Heijnen *et al.* model.

On the other hand, the family of production kinetics (12) is sufficiently smooth to guarantee the applicability of this theorem. For the original model we prove the following theorem.

Theorem 1

Consider the minimization of performance index (8) subject to the dynamic constraint (6). Suppose that the specific rates are modelled by equations (2)–(4) which are continuous piecewise smooth functions of the substrate concentration. Then during singular control the substrate concentration remains constant if and only if the hydrolysis constant $k_h = 0$ and is

determined by the equation

$$\mu = \mu_{\text{crit}}$$

This constant value maximizes the yield π/σ .

Proof. In the following a prime denotes derivation with respect to substrate concentration C_s . For every value of the parameter B in the half open interval $]0, \mu_{\text{crit}}]$ the specific rates (2), (4) and (12) are smooth functions of the substrate concentration C_s only. In this case we know that on the singular interval C_s remains constant if and only if $k_h = 0$.⁴ C_s satisfies

$$\pi' \sigma - \sigma' \pi = 0 \quad (18)$$

We have

$$\frac{d\pi}{dC_s} = \frac{d\pi}{d\mu} \frac{d\mu}{dC_s}$$

By using equation (4) in the form

$$\frac{d\mu}{dC_s} = Y_{x/s} \left(\frac{d\sigma}{dC_s} - \frac{1}{Y_{p/s}} \frac{d\pi}{dC_s} \right)$$

we obtain a relation between π' and σ' which can be written as

$$\pi' = F(\mu, B) \sigma' \quad (19)$$

with

$$F(\mu, B) \triangleq \frac{Q_{p,\max} Y_{x/s} [1 - (\mu - \mu_{\text{crit}} + 2B)/R(\mu, B)] / 2(\mu_{\text{crit}} - B)}{1 + Q_{p,\max} Y_{x/s} [1 - (\mu - \mu_{\text{crit}} + 2B)/R(\mu, B)] / 2(\mu_{\text{crit}} - B) Y_{p/s}}$$

$$R(\mu, B) \triangleq \sqrt{[(\mu + \mu_{\text{crit}})^2 - 4(\mu_{\text{crit}} - B)\mu]}$$

Substituting (19) in (18) and noting that $\sigma' \neq 0$, we obtain

$$F(\mu, B) \left(\frac{\mu}{Y_{x/s}} + m + \frac{\pi}{Y_{p/s}} \right) = \pi$$

We now follow a similar line of reasoning (based on Conjecture 1) as used in the determination of the optimal control for the model involving the original kinetics (3) starting from a model with smooth kinetics (12). Thus we consider the limit for $B \rightarrow 0$ on both sides of the above equation to obtain

$$Y_{x/s} [|\mu - \mu_{\text{crit}}| - (\mu - \mu_{\text{crit}})] \left(\frac{\mu}{Y_{x/s}} + m + \frac{Q_{p,\max}}{2Y_{p/s}\mu_{\text{crit}}} (\mu + \mu_{\text{crit}} - |\mu - \mu_{\text{crit}}|) \right)$$

$$= (\mu + \mu_{\text{crit}} - |\mu - \mu_{\text{crit}}|) \left(|\mu - \mu_{\text{crit}}| + \frac{Y_{x/s} Q_{p,\max}}{2Y_{p/s}\mu_{\text{crit}}} [|\mu - \mu_{\text{crit}}| - (\mu - \mu_{\text{crit}})] \right)$$

Solving for μ obviously leads to

$$\mu = \mu_{\text{crit}}$$

Using equation (4), the substrate concentration during singular control is

$$C_{s,\text{sing}} = K_s \frac{\mu_{\text{crit}}/Y_{x/s} + m + Q_{p,\max}/Y_{p/s}}{Q_{s,\max} - (\mu_{\text{crit}}/Y_{x/s} + m + Q_{p,\max}/Y_{p/s})} \equiv C_{s,\text{crit}}$$

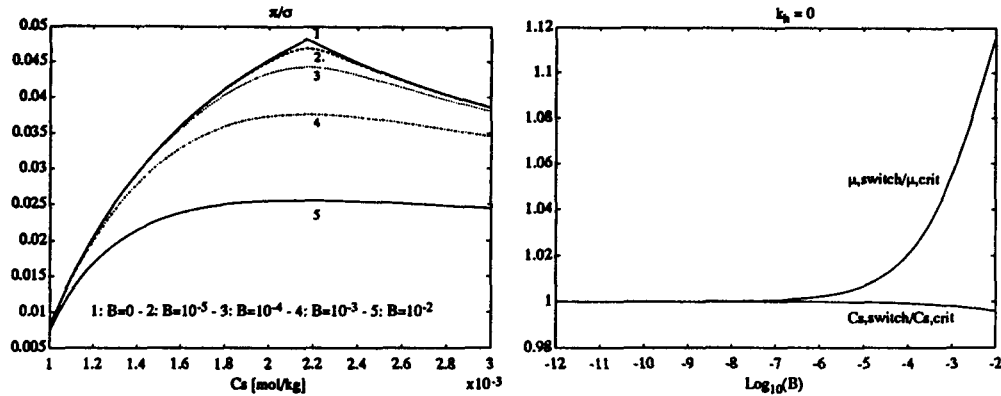


Figure 7. Left plot: π/σ as a function of C_s for various values of B . Right plot: optimal switch values for μ and C_s as a function of B with $k_h = 0$

The left plot of Figure 7 shows values of π/σ as a function of C_s for different values of B . We conclude that for $B = 0$, π/σ takes on its maximum value at $C_s = C_{s,\text{crit}}$. \square

Observe that for $B = \mu_{\text{crit}} = 10^{-2}$, π/σ exhibits a (very smooth) maximum, corresponding to a finite value of $C_{s,\text{switch}}$. This is an additional verification that the optimal control in this case is not a simple batch process while adding all available substrate α at $t = 0$ as might have been expected. In the right plot of Figure 7 we show the optimal value for μ and the corresponding value of C_s (calculated using (18)) at which to switch from batch to singular control for different values of B with $k_h = 0$. Observe the convergence to $\mu \rightarrow \mu_{\text{crit}}$ and $C_s \rightarrow C_{s,\text{crit}}$ when $B \rightarrow 0$ as indicated by Theorem 1. These plots illustrate again that setting $B = 10^{-11}$ in (12) is a very accurate approximation of the original kinetics (3).

In general, hydrolysis $k_h \neq 0$, so we do not know the switch time t_2 in *closed-loop* form, i.e. as function of state variables only. However, the above theorem provides a good initial guess for t_2 if k_h is sufficiently small. It also indicates that during singular control the substrate concentration will be time-varying. Obviously, for k_h small the variations in C_s with respect to t will also be small, as illustrated by the simulation results presented earlier.

5. HEURISTIC CONTROL STRATEGIES

5.1. Suboptimal control strategies

In this section we propose *heuristic* control strategies based on microbial and mathematical knowledge. We also indicate the conditions under which the suboptimal solution coincides with the *optimal* one.

In contrast with the optimal control approach, there will be no need for partial derivatives. Thus the original model ($B = 0$) can be handled directly without any difficulty: as a matter of fact, the presence of a corner in the production kinetics (3) facilitates the design of a suboptimal controller.

From the *microbiological and experimental* point of view the construction of a suboptimal profile can be based on the concept of a *biphasic* fermentation process.

5.1.1. Growth phase $[0, t_2]$. During the growth phase we focus on the specific growth rate

μ in (4). For the control needed we refer to the optimal control results: in the case of an unbounded input and an unconstrained state vector the growth phase is a *batch* phase. All substrate consumed for growth is added all at once at time $t = 0$ in order to obtain the highest possible value of μ . Note that for the original specific production rate (3) this results in maximizing π also. In the case of a constraint on the input and/or the state some minor modifications are required.

5.1.2. *Production phase* $[t_2, t_3]$. During production we focus on the specific production rate π .

- (i) *Original model*. Equation (3) indicates that the lowest value of μ which still guarantees the maximum value of π is $\mu = \mu_{\text{crit}}$. Note that this is equivalent to $C_s = C_{s,\text{crit}}$, so the control during production is of the form

$$u_{\text{production}}(t) = \frac{C_{s,\text{in}}\sigma X}{C_{s,\text{in}} - C_s} \quad (20)$$

maintaining C_s and thus μ at their critical values. This choice can also be motivated from the analysis of the optimal control result (see Figure 4). As a consequence, the conjunction point t_2 of growth and production follows from the condition:

$$C_s(t_2) = C_{s,\text{crit}} \quad \text{or} \quad \mu(t_2) = \mu_{\text{crit}}$$

The control (20) is stopped at $t = t_3$ when all substrate is used (see (9) and (10)). As in the optimal case, the final *batch* phase $[t_3, t_f]$ is stopped when $dP/dt = 0$. Note that the complete suboptimal control is obtained in *closed loop* for a given initial substrate amount S_0 . As a result, the optimization problem is reduced to the *one-dimensional optimization of S_0* .

- (ii) *Modified model*. For values of B in the interval $0 < B \leq \mu_{\text{crit}}$ it is less clear how to determine a heuristic control during production, since the specific production rate π in (12) no longer has a corner point. However, we will verify that keeping C_s and thus μ *constant* using a control of the form (20) is an appropriate choice for this case also. The switch from growth to production can be determined as follows. As a first guess we can still switch on $C_s = C_{s,\text{crit}}$ and thus $\mu = \mu_{\text{crit}}$. However, we know from Section 4 and Figure 7 that this guess is only appropriate for B near zero. For B near μ_{crit} we will simply optimize the switch time t_2 . As in the optimal control case, we obtain a *two dimensional optimization of S_0 and t_2* .

As a *mathematical justification*, it follows immediately from Theorem 1 that the suboptimal control profile for the original model reduces to the optimal profile if (and only if) $B = 0$ and $k_h = 0$.

Before giving some simulation results, some advantages of these suboptimal profiles are mentioned. It is well known that putting an optimal control into practice may be hampered by a lot of problems. Since optimal control is a very model-sensitive technique, a feedforward will not generate the predicted simulation results. As long as a sufficiently accurate model for the penicillin fermentation is not available, the determined optimal control profiles can be used only to obtain a greater qualitative insight to the process.

On the other hand, the *suboptimal* profiles we present here are the translation of a more realistic control objective, namely *setpoint* control, for which even adaptive control algorithms can be developed. It is illustrated in References 3 and 4 that we could keep the specific growth rate μ constant *without* the knowledge of an exact analytic expression for it, so the controller

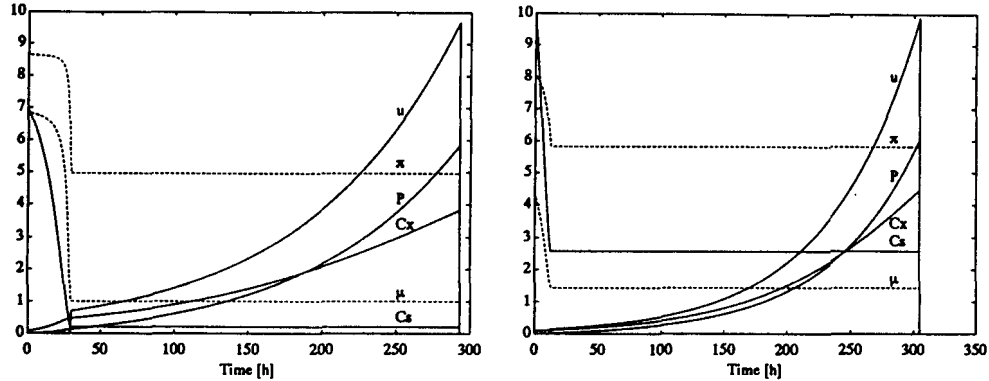


Figure 8. $B = \mu_{\text{crit}} = 10^{-2}$. Suboptimal glucose feed rate and corresponding cell, glucose, product, π - and μ -profiles. Left plot: $\mu_{\text{switch}} = \mu_{\text{crit}}$. Scaling: $C_s \times 10^2$, $C_x \times 2$, $P/750$, $\mu \times 100$, $\pi \times 3 \times 10^4$, $u/220$. Right plot: μ_{switch} free. Scaling: $C_s \times 10^3$, $C_x \times 2$, $P/750$, $\mu \times 100$, $\pi \times 3 \times 10^4$, $u/300$.

becomes model-independent. Furthermore, there would be no need for a complete measurement of the state, a problem which has not been solved completely up to now.

5.2. Simulation results

5.2.1. $B = 10^{-11}$. Some numerical values are summarized in Table II. From these we conclude that for the original model the *suboptimal control results almost coincide with the optimal values* thanks to the low value of k_h .

5.2.2. $B = \mu_{\text{crit}} = 10^{-2}$. For $\pi(\mu)$ modelled by the Monod-type kinetics (13) the results are summarized in Table II and Figure 8. We have done the optimization with $\mu_{\text{switch}} = \mu_{\text{crit}}$ (left plot) and μ_{switch} considered *free* (right plot). Note that — in contrast with the *optimal* profiles shown in Figure 5 — for both suboptimal profiles there is still an initial batch phase. For $\mu_{\text{switch}} = \mu_{\text{crit}}$ the final amount P_f reaches 96.39% of the optimal value. For μ_{switch} considered *free* we obtain as much as 99.77% of the optimal value. These results sufficiently illustrate the performance of the suboptimal profiles over the whole range of parameter B .

Remark. Although the only model reported in the literature is the one with $B = 0$, we also presented some simulation results for other values of B . This can be motivated as follows. First of all, from the biochemical point of view a sharp corner in π at $\mu = \mu_{\text{crit}}$ is of course only a first approximation of real-life fermentation conditions. Thus a value for B different from zero seems more realistic. Secondly, these results make it possible to illustrate the convergence of the controls to the desired one following the basic Conjecture 1; see e.g. Figure 6. Finally, they confirm the use of the developed algorithms for optimal and suboptimal control not only for the original models but also for the whole class of models considered.

6. CONCLUSIONS

We can extract the following results from the application of optimal control theory to the penicillin G fed-batch fermentation process by using the unstructured mathematical model of Heijnen *et al.*⁵ and a newly developed modified version.

1. We verified and confirmed the statement by Heijnen *et al.* that the *glucose feed scheme is of crucial importance in obtaining high penicillin yields*. In order to do so, we determined for the first time the optimal control profile for a well-defined optimization problem using their model and the modified version. We have shown that the obtained control generates the global optimum of the performance measure under consideration, using a straightforward computational algorithm. Simulation results indicated a possible gain of several hundred per cent as compared with the outcome of a constant control input with zero initial substrate amount for the same time. Furthermore, this model is very sensitive towards different feeding policies.
2. From the mathematical point of view we presented the application of a new, elegant conjecture that allows for the determination of optimal control profiles for a class of piecewise smooth models that cannot be handled using standard optimal control theory. Since this kind of model is not limited to the biotechnological field itself, this procedure can be of great use in a lot of other scientific domains also. Furthermore, we were able to include the optimization of some initial states in the resulting two-point boundary value problem.
3. In the field of model building, the results obtained using optimal control theory indicated some possible shortcomings in the model used, without carrying out any costly and time-consuming experiments. The combination of the enormous gains in production and the vanishing of the characteristic biphasic behaviour through optimization led us to conclude that the present model might be less useful for advanced control purposes than suggested by Heijnen *et al.*⁵ In this way this optimal control study can prove to be very useful for model discrimination purposes: *optimization for model discrimination*. This motivates a deeper study of this model presented in Reference 4.
4. We have shown that the heuristic control algorithms developed in Section 5 are a successful alternative for the optimal control using essentially the same computational algorithm for the whole family of models considered. From the characterization of the singular arc in the optimal control solution, we derived conditions under which this heuristic strategy coincides with the optimal control. It is shown in References 3 and 4 that these suboptimal controllers can serve indeed as a basis for the development of model-independent control algorithms: *optimal adaptive control*.

ACKNOWLEDGEMENTS

This research has been partially performed under the Belgian National Incentive Program on Fundamental Research in Life Sciences initiated by the Belgian State, Prime Minister's Office, Science Policy Programming. The scientific responsibility is assumed by its authors. The authors are also grateful to Dr D. Dochain of the Université Catholique de Louvain, Louvain-la-Neuve, Belgium for his stimulating comments. Jan Van Impe is a senior research assistant and Bart De Moor a research associate with the Belgian National Fund for Scientific Research (N.F.W.O.).

REFERENCES

1. Bastin, G., 'Nonlinear and adaptive control in biotechnology: a tutorial', *Proc. 1991 Eur. Control Conf.* (Grenoble), Hermes, Paris, 1991, pp. 2001–2012.
2. Bastin, G., and D. Dochain, *On-line Estimation and Adaptive Control of Bioreactors*, Elsevier, Amsterdam, 1990.

3. Van Impe, J. F., G. Bastin, B. De Moor, V. Van Breusegem and J. Vandewalle, 'Optimal adaptive control of fed-batch fermentation processes with growth/production decoupling', in M. N. Karim and G. Stephanopoulos (eds.), 'Modeling and control of biotechnical processes', Pergamon Press, Oxford, 1992, p. 351-354.
4. Van Impe, J. F., *Modeling and Optimal Adaptive Control of Biotechnological Processes*, Ph.D. Thesis, Department of Electrical Engineering, Katholieke Universiteit Leuven, 1993.
5. Heijnen, J. J., J. A. Roels and A. H. Stouthamer, 'Application of balancing methods in modeling the penicillin fermentation', *Biotechnol. Bioeng.*, **21**, 2175-2201 (1979).
6. Bajpai, R. K. and M. Reuß, 'A mechanistic model for penicillin production', *J. Chem. Technol. Biotechnol.*, **30**, 332-344 (1980).
7. Van Impe, J. F., B. M. Nicolai, J. A. Spriet, B. De Moor and J. Vandewalle, 'Optimal control of the penicillin G fed-batch fermentation: an analysis of the model of Bajpai and Reuß', in Mosekilde, E., (ed.), *Modelling and Simulation 1991*, Society for Computer Simulation SCS, San Diego, CA, 1991, p. 867-872.
8. Spriet, J. A., 'The control of fermentation processes', *Med. Fac. Landbouww. Rijksuniv. Gent*, **52**, (4), 1371-1381 (1981).
9. Roels, J. A., *Energetics and Kinetics in Biotechnology*, Elsevier, Amsterdam, 1983.
10. Modak, J. M., H. C. Lim and Y. J. Tayeb, 'General characteristics of optimal feed rate profiles for various fed-batch fermentation processes', *Biotechnol. Bioeng.*, **28**, 1396-1407 (1986)
11. Fishman, V. M., and V. V. Biryukov, 'Kinetic model of secondary metabolite production and its use in computation of optimal conditions', *Biotechnol. Bioeng. Symp.*, **4**, 647-662 (1974).
12. Athans, M., and P. L. Falb, *Optimal Control*, McGraw-Hill, New York, 1966.
13. Bryson Jr., A. E. and Y.-C. Ho, *Applied Optimal Control*, Hemisphere, Washington, DC 1975.
14. Van Impe, J. F., B. Nicolai, P. Vanrolleghem, J. Spriet, B. De Moor and J. Vandewalle, 'Optimal control of the penicillin G fed-batch fermentation: an analysis of a modified unstructured model', *Chem. Eng. Commun.*, **117**, 337-353 (1992).
15. Lim, H. C., Y. J. Tayeb, J. M. Modak and P. Bonte, 'Computational algorithms for optimal feed rates for a class of fed-batch fermentation: numerical results for penicillin and cell mass production', *Biotechnol. Bioeng.*, **28**, 1408-1420 (1986).